The Canadian Mineralogist
Vol. 48, pp. 483-495 (2010)
DOI: 10.3749/canmin.48.3.483

THE CRYSTAL STRUCTURE OF 7H : 12Q CANNIZZARITE FROM VULCANO, ITALY

DAN TOPA[§]

Department of Materials Research and Physics, Paris-Lodron University of Salzburg, Hellbrunnerstrasse 34, A–5020 Salzburg, Austria

EMIL MAKOVICKY

Department of Geography and Geology, University of Copenhagen, Østervoldgade 10, DK–1350, Copenhagen, Denmark

HERBERT DITTRICH

Department of Materials Research and Physics, Paris-Lodron University of Salzburg, Hellbrunnerstrasse 34, A–5020 Salzburg, Austria

ABSTRACT

The crystal structure of cannizzarite, ideally $Pb_{48}Bi_{56}(S_{124}Se_8)_{132}$, a fumarole sublimate from the La Fossa crater, on the island of Vulcano, Italy, with a nominal composition $Pb_{47.9}Bi_{55.8}(S_{121.8}Se_{10.5})_{\Sigma 132.3}$ and unit-cell parameters *a* 38.86(3), *b* 4.090(3), *c* 39.83(3) Å, β 102.30(3)°, *Z* = 1, has been solved and refined in space group $P2_1/m$ from X-ray single-crystal diffraction data, to an R_1 of 10.7% on the basis of 3612 unique reflections with $[F_o > 4\sigma(F_o)]$; the data were collected on a Bruker P3 diffractometer with a CCD detector and Mo*K*α radiation.The cannizzarite crystal studied has 104 cations and 132 anions in a unit cell. Refinement shows that about eight anions per cell contents are selenium, the bulk being sulfur. The crystal structure is composed of pseudotetragonal layers (Q layers), two cation–anion planes thick, of the $(100)_{PbS}$ type that alternate with double-octahedron pseudohexagonal layers (H layers) of the $(111)_{PbS}$ type. Both types of layer contain Pb and Bi; their distribution was studied by means of bond-valence calculations, polyhedron characteristics and bond-length ratios of the opposing *Me*–anion bonds. The unit-cell contents are $Me_{48}X_{48}$ for the Q layers, and $Me_{56}X_{84}$ for the H layers. Selenium was found only in H layers. The structure determined represents the shorter of the two modules, $Pb_{12}Bi_{14}S_{33}$ and $Pb_{17}Bi_{20}S_{47}$, found in the structure of synthetic cannizzarite proposed earlier, and proves their independent existence.

Keywords: sulfosalt, cannizzarite, crystal structure, La Fossa, Vulcano, Italy.

SOMMAIRE

Nous avons résolu et affiné la structure cristalline de la cannizzarite, de formule idéale $Pb_{48}Bi_{56}(S_{124}Se_8)_{132}$, ayant une composition globale $Pb_{47.9}Bi_{55.8}(S_{121.8}Se_{10.5})_{\Sigma 132.3}$ et les paramètres réticulaires *a* 38.86(3), *b* 4.090(3), *c* 39.83(3) Å, β 102.30(3)°, *Z* = 1, groupe spatial $P2_1/m$. Le minéral a été prélevé sur les parois d'une fumerolle au cratère La Fossa, île de Vulcano, en Italie. Le traitement des données en diffraction X, prélevées sur monocristal, ont été enregistrées avec un diffractomètre Bruker P3 muni d'un détecteur CCD et utilisé avec rayonnement Mo*K*α, et ont mené à un résidu R_1 de 10.7% sur une base de 3612 réflexions uniques $[F_o > 4\sigma(F_o)]$. Le cristal étudié contient 104 cations et 132 anions par maille. L'affinement montre qu'environ huit anions par maille sont des atomes de sélénium, le reste étant du soufre. La structure est composée de couches pseudotétragonales (Q) d'une épaisseur de deux liaisons cation–anion de type $(100)_{PbS}$ qui alternent avec une couche pseudohexagonale (H) d'octaèdres doubles de type $(111)_{PbS}$. Les deux sortes de couches contiennent Pb et Bi; nous en avons étudié leur distribution au moyen de calculs de valences de liaison, des caractéristiques des polyèdres, et des rapports de longueurs des liaisons *Me*–anion opposantes. La maille élémentaire contient $Me_{48}X_{48}$ dans les couches Q, et $Me_{56}X_{84}$ dans les couches H. Le sélénium ne se trouve que dans les couches H. La structure déterminée représente le plus court des deux modules, $Pb_{12}Bi_{14}S_{33}$ et $Pb_{17}Bi_{20}S_{47}$, décrits antérieurement dans la structure de la cannizzarite synthétique, ce qui prouve ainsi leur existence indépendante.

(Traduit par la Rédaction)

Mots-clés: sulfosel, cannizzarite, structure cristalline, cratère La Fossa, Vulcano, Italie.

§ *E-mail address*: dan.topa@sbg.ac.at

Introduction

Cannizzarite, a Pb–Bi sulfosalt with a nominal composition $Pb_{46}Bi_{54}(S,Se)_{127}$, is a product of fumarole exhalations at the crater of La Fossa, the island of Vulcano, Aeolian Islands, southern Italy. It was described by Zambonini *et al*. (1924). Its crystallography was studied by Graham *et al*. (1953) by means of single-crystal X-ray diffraction, and the crystal structure was determined by Matzat (1979a, b), who examined both natural and synthetic material. Electron-microprobe studies of its composition were performed by Mozgova *et al*. (1984, 1988, 1992) on material from Vulcano and Siberia, and by Mumme (1980) and Mozgova *et al*. (1992) on the related material, "wittite", with an elevated Se:S ratio. Several hydrothermal-metamorphic assemblages with Se-free cannizzarite have been described from Switzerland, *e.g*., by Nowacki & Stalder (1969) and Berlepsch *et al*. (2001), whereas Topa *et al*. (2001) described a sample of selenium-free cannizzarite from a hydrothermal-metamorphic assemblage at Felbertal, Austria. High-resolution TEM studies of cannizzarite were performed by Williams (1986). Up-to-date data on cannizzarite were summarized by Makovicky & Hyde (1981, 1992). The most recent study of this mineral is by Borodaev *et al*. (2000). Mozgova *et al*. (1992) and Borodaev *et al*. (2000) used electron microdiffraction for identification of the material. Zhang *et al*. (2005) studied the crystal structure of a synthetic selenian member of this structural family, $Pb_5Bi_6Se_{14}$.

In spite of the intensive research on cannizzarite quoted above, the only crystal-structure determination published is that by Matzat (1979a, b), on a synthetic material. In his work, he postulated that the structure obtained can be described as a combination of two long-range modules ("unit verniers"), one of which has been found *in a pure form* in the present study. Thus, our results confirm that cannizzarite is not a single mineral but a *variable-fit homologous series* of closely related phases (Makovicky 1988, Ferraris *et al*. 2004). Their presence has serious implications for a compositional range of this series. Until further crystal-structure determinations have been performed, especially on the other "pure" module postulated by Matzat (1979a, b), any speculations on the range and compositional limits of cannizzarite, especially those based solely on electron-microprobe data on this "mineral", extremely difficult to analyze because of its morphology, are considered premature.

General Properties and Selected Results of Previous Studies

The crystal structure of cannizzarite is composite, consisting of an alternation of pseudotetragonal (Pb,Bi)(S,Se) layers (denoted below as Q layers) and double-octahedron $(Pb,Bi)_2(S,Se)_3$ pseudohexagonal layers (H layers). The latter were compared by Moëlo *et al*. (2008) with similar layers in tetradymite and its isotypes. The layers are commensurate in one intralayer direction (which displays a 4 Å period), but they are noncommensurate in the other intralayer direction, perpendicular to the previous one, producing only a 1D long-range match, and possibly only an empirical one.

Local structures of the component layers generate strong subperiods, expressed by two subcells, a pseudotetragonal one and a centered orthohexagonal (*i.e*., pseudohexagonal) one. In the direction of the long-range match, the two subperiods are about 4.1 and 7.0 Å, respectively, in contrast to the common period, about 4.1 Å in the direction perpendicular to the long-range match, and the layer-stacking period, about 15.5 Å. The concept of subcells allows one to express the observed match of the two component layers in simple terms (Matzat 1979a, b, Makovicky & Hyde 1981, 1992).

The studies of Matzat (1979a, b) suggest that the complex structure of cannizzarite, with intralayer periods reaching 189.8 Å in the natural material and ~169 Å in the synthetic sample, can be approximated by an alternation of simpler blocks (*i.e*., modules with simpler H:Q matches) that combine in different proportions along the long-range direction. The smaller block has an internal (*model*) match of seven centered pseudohexagonal (H) subcells with 12 primitive pseudotetragonal (Q) subcells, whereas in the other block, 10 H subcells match the length of a Q segment with 17 Q subcells. Model compositions of these two modules are $Pb_{12}Bi_{14}S_{33}$ and $Pb_{17}Bi_{20}S_{47}$, respectively, if one assumes full site-occupancies and the occurrence of these modules as independent structures. In the real long-range structure, they are only approximate, and the true match (if it is not only empirical in nature) ought to be only the one in the resulting composite. More on this topic can be found in the compilation by Makovicky & Hyde (1981, 1992) and in Ferraris *et al*. (2004). At such spacings, measurement errors can influence the results substantially, and cannizzarite is the best potential candidate sulfosalt for a structure composed of two truly non-commensurate sets of alternating layers. On the contrary, the layer match in the synthetic selenian analogue, $Pb_5Bi_6Se_{14}$ (Zhang *et al*. 2005) seems to be of the shortest possible type, 5Q : 3H subcells. Recent results on synthetic tin–selenium cylindrite by Makovicky *et al*. (2008) reveal an interesting and complex relationship between the subcell match and the period of transversal modulation; its bearing upon the situation in cannizzarite is not immediately obvious, however.

Although Graham *et al*. (1953) quoted diffraction results in agreement with the presence of a smaller module alone, no recent acquisition of data or crystal-structure determination has been performed on either of the two "component modules" of cannizzarite defined above. Therefore, our study of one of these "block"

structures, presented here, on a natural material is the first step in elucidating the interesting modular aspect of cannizzarite. The diffraction data recorded suggest the presence of (at least empirical) long-range commensurability of the two component layer-sets in the sample studied, as indicated by the unit cell refined. Therefore, a classical commensurate refinement appears justified, even if the match may perhaps be an empirical one. A subsequent modulated refinement approach in a four-dimensional space will be a very welcome alternative, especially for sorting out the transversal modulation waves acting on the component layers. These are much less pronounced and appear more complex than the transversal modulation waves, *e.g.*, in cylindrite (Makovicky *et al*. 2008).

Experimental

Chemical data

The material studied comes from volcanic fumaroles of the active volcanic crater La Fossa, on the island of Vulcano, Italy. We investigated a portion of the specimen with inv. no II/2298 from the Mineral Collection of the Institute of Mineralogy, which was acquired around the mid-80s from Mr. G. Gebhard's collection. We have no indication about the acquisition time of the sample. Quantitative electron-microprobe analyses of a polished section prepared from free crystals and aggregates of sulfosalts were performed with JEOL Superprobe JXA–8600, controlled by Probe for Windows system of programs, operated at 25 kV and 35 nA (measurement times of 15 s for peak and 5 s for background), installed at the Department of Geography and Geology, University of Salzburg. The following standards and X-ray lines were used: natural $CuFeS_2$ (chalcopyrite; Cu$K\alpha$), natural PbS (galena Pb$L\alpha$), synthetic Bi_2S_3 (Bi$L\alpha$, S$K\alpha$), synthetic Bi_2Se_3 (Se$L\alpha$), synthetic CdTe (Cd$L\beta$) and Ag metal (Ag$L\alpha$). The raw data were corrected with the on-line ZAF-4 procedure. Silver, cadmium and copper contents are below detection limits in analyzed grains, in contrast with the chemical composition of cannizzarite from Felbertal, which contains 1.1 wt.% Ag, 1.0% Cd, and 0.2% Cu, related to higher Bi and lower Pb concentrations. The mean result of our four best electron-microprobe analyses of cannizzarite, 37.79(12)% Pb, 44.44(20)% Bi, 3.15% Se and 14.88(4)% S [total 100.26(16)%], result in the formula $Pb_{47.88(16)}Bi_{55.83(24)}Se_{10.46(16)}S_{121.83(28)}$ calculated for 236 atoms in a unit cell. If the formula is calculated for the sum of cations in the unit cell equal to 104 cations, the formula becomes $Pb_{48.01(16)}Bi_{55.99(24)}Se_{10.49(16)}S_{122.17(28)}$. This formula can be compared with that derived from the crystal-structure determination, $Pb_{48}Bi_{56}Se_8S_{124}$. The largest difference is, as expected, in the presence of many mixed-anion sites, in the Se:S ratio and in the sum of anions, X = 132.66 instead of 132 (an absolute error of 0.5%).

Single-crystal diffraction

For our single-crystal investigation, elongate, lath-like almost free crystals were picked directly from the hand specimen. They were investigated with a Bruker AXS P3 diffractometer equipped with a CCD area detector using graphite-monochromated Mo$K\alpha$ radiation. Because of its lath-like shape, with crystals generally bent and split during growth, forming chaotic intergrowths in form of loose crusts, and because of twinning, softness as well as cleavage, finding a suitable crystal of cannizzarite is a tedious task. The irregular fragment we selected measured approximately 0.01 × 0.03 × 0.15 mm. Experimental data are listed in Table 1. The Smart (Bruker AXS, 1998) system of programs was used for unit-cell determination and data collection, Saint+ (Bruker AXS, 1998), for the calculation of integrated intensities, and Xprep (Bruker AXS, 1998), for empirical absorption-correction based on pseudo Ψ-scans. The space group is $P2_1/m$, as proposed

TABLE 1. SINGLE-CRYSTAL X-RAY DIFFRACTION OF CANNIZZARITE: EXPERIMENTAL AND REFINEMENT DETAILS

Crystal data

Chemical formula	$Pb_{48}Bi_{56}S_{124}Se_8$	Formula weight	15523
Crystal system	Monoclinic	Space group	$P2_1/m$
a (Å)	38.869(29)	D_x (mg m^{-3})	6.97
b (Å)	4.090(3)	No.of reflections for cell param.	1926
c (Å)	39.835(33)	μ (mm^{-1})	62.2
β (°)	102.30(3)	Crystal shape	needle-like
V (Å^3)	6188(4)	Crystal color	black
Z	1		
Crystal size (mm)	0.01 × 0.03 × 0.15		

Data collection

T_{min}	0.29	T_{max}	0.99
No. of measured reflections		18664	
No. of independent reflections		12979	
No. of observed reflections		3612 for $F_o > 4\sigma(F_o)$	
Criterion for observed reflections		$I > 2\sigma(I)$	
R_{int}, R_{sigma}		17.8, 16.4%	
θ_{max} (°)		28.3	
Range of h, k, l		-50 ≤ h ≤ 27, -4 ≤ k ≤ 5, -30 ≤ l ≤ 42	

Refinement

Refinement on F_o^2 R_1 [$F_o > 4\sigma(F_o)$]	10.73%
$wR(F_o^2)$	25.58%
S (*GooF*)	0.911
No. of reflections used	3612
No. of parameters refined	530
Weighting scheme	$w = 1/[\sigma^2(F_o^2) + (0.1366P)^2+0.0P]$, where $P = (F_o^2 + 2F_c^2) / 3$
$(\Delta / \sigma)_{max}$	0.003
$\Delta\rho_{max}$ (e/Å^3)	6.17 [0.93 Å from Bi26]
$\Delta\rho_{min}$ (e/Å^3)	–6.80 [1.02 Å from Bi21]
Extinction coefficient	0.000002(3)

Source of atomic scattering factors: *International Tables for Crystallography* (1992, Vol. C, Tables 4.2.6.8 and 6.1.1.4)

Computer programs

Structure solution	*SHELXS97* (Sheldrick 1997a)
Structure refinement	*SHELXL97* (Sheldrick 1997b)

by the XPREP program. The structure was solved by direct methods (program SHELXS by Sheldrick 1997a) and difference-Fourier syntheses (program SHELXL by Sheldrick 1997b). Data on X-ray diffraction and structure refinement are summarized in Table 1. With 3265 accepted unique reflections and 560 refined parameters (anisotropic displacement parameters for cations and isotropic ones as well as S, Se occupancy factors for anions), the R_1 value is 10.7%, chiefly in connection with the quality of the data obtainable (R_{int} after absorption correction of this highly absorbing material is 17.8%). Positional and displacement parameters refined are in Table 2, selected interatomic distances in Table 3, and coordination-polyhedron characteristics calculated with IVTON program (Balić-Žunić & Vicković 1996), in Table 4. A table of structure factors may be obtained from the Depository of Unpublished Data on the Mineralogical Association of Canada website [document Cannizzarite CM48-483]. The crystal structure is illustrated in Figures 1 and 2.

CRYSTALLOGRAPHY

Single-crystal diffraction data indicate that the crystal of cannizzarite studied has unit-cell parameters *a* 38.86(3), *b* 4.090(3), *c* 39.83(3) Å, β 102.30(3)°, space group $P2_1/m$. The Q and H layers of the structure are parallel to $(10\bar{1})$, so that the *a* and *c* parameters span the interlayer spaces, and the *b* parameter is an intralayer vector. The length of a layer-stacking vector in then 15.165 Å for one Q–H pair, obtained by *averaging* over four pairs along $[10\bar{1}]$. The weighted reciprocal lattice of cannizzarite can be divided into contributions from the pseudotetragonal component, those from the pseudohexagonal component ("the two sublattices"), and the common modulation reflections. If the two sublattices were not matching in the above mentioned ratio 7H : 12Q, a "forced" common cell would definitely have high standard deviations for its cell parameters; they would then be much higher than observed.

CRYSTAL STRUCTURE

Our determination of the structure indicates 52 independent cation sites and 66 independent anion sites (Table 2), *i.e.*, 104 cations and 132 anions in a unit cell. All atoms are situated at *y* equal to ¼ or ¾, with positions general in the *x*–*z* plane. Our refinement shows that of the 66 anion sites, 14 anion sites are (S,Se) mixed sites (two around 50:50, seven around 75:25 and five around 90:10). In other words, about eight anions *per* cell contents are selenium, the bulk being sulfur (Table 2, Figs.1, 2). All these sites are located in the H layers. There are several sulfur positions in the structure with U_{iso} close to zero (Table 2). These are the sites with potential small contents of selenium substituting for sulfur, augmenting in this way the selenium content in the structure-derived formula, bringing it closer to the results of the electron-microprobe analyses.

The total composition for the Q component is $Me_{48}X_{48}$, that for the H layers is $Me_{56}X_{84}$ in a cell. Coordination analysis (Table 4) suggests that of 24 independent cation positions in the Q layers, 13 are (predominantly) Pb, nine are Bi, and only two (*Me*11 and *Me*13) are mixed sites. Separation is much less obvious in the H layers, in which only six Pb sites and 12 Bi sites might be relatively pure, not mixed-cation sites. The remaining 11 sites are mixed sites, some with more Pb, others with more Bi, or about evenly mixed (Table 4, Fig. 2).

A more detailed coordination-state analysis of the distribution of cations in both sets of layer was performed by means of bond-length ratio hyperbolae (Trömmel 1981) in a way described in detail by Berlepsch *et al.* (2001a, b). For the H component (Fig. 3a), typical lead sites are *Me*25, 37 and 47, typical mixed sites are, *e.g.*, *Me*34, 41, 42 and 43, whereas sites with strongest indication of Bi are *Me*27, 38, and 48, and especially *Me*50. In Figures 3a and b, the bond-length ratios of opposing bonds are divided into the "in-plane" and "out-of-plane" sets; the former describes the bonding situation in the base of the "square" coordination pyramid MeX_5, whereas the latter combines the bond length to the vertex of the pyramid with an additional, long *Me*–S distance below the base. They are plotted into the opposing sectors of the diagram, divided by its diagonal. For the H layers of the cannizzarite sample studied, the bulk distribution of data points describing the cations is symmetrical about the line separating the in-plane and out-of-plane bonds distances (Fig. 3a). This apparently is a product of bond distribution: the character and length of the long below-plane bonds are influenced by their orientation inward, toward the median plane of the double-octahedron H layer, and not into "free" interlayer space, and the outwardly oriented (generally shorter) bonds in many cases are bonds to mixed S,Se positions, *i.e.*, they are longer than expected for such bonds. The presence of split cation positions, with two alternative, partly occupied cation sites in the same coordination polyhedron, expressed as in-plane flipping of some cations in the square base of the coordination pyramid, is probable for those cations (especially in the mixed sites) for which the in-plane data points plot close to the median line. However, evaluation of this aspect is made difficult by the presence of mixed *Me*–(S,Se) bonds on the short-bond side of the bond-length ratio.

The Q layers show a fairly distinct distribution of the (predominantly) Bi and (predominantly) Pb positions in Figure 3b. The clear 1:1 mixed sites are only the *Me*11 and *Me*13 sites. Interlayer Pb–S and Bi–S distances seen for different coordination polyhedra of the Q layer are rather uniform. This, perhaps, is a result of an overall compromise in configuration (a uniform diameter) of

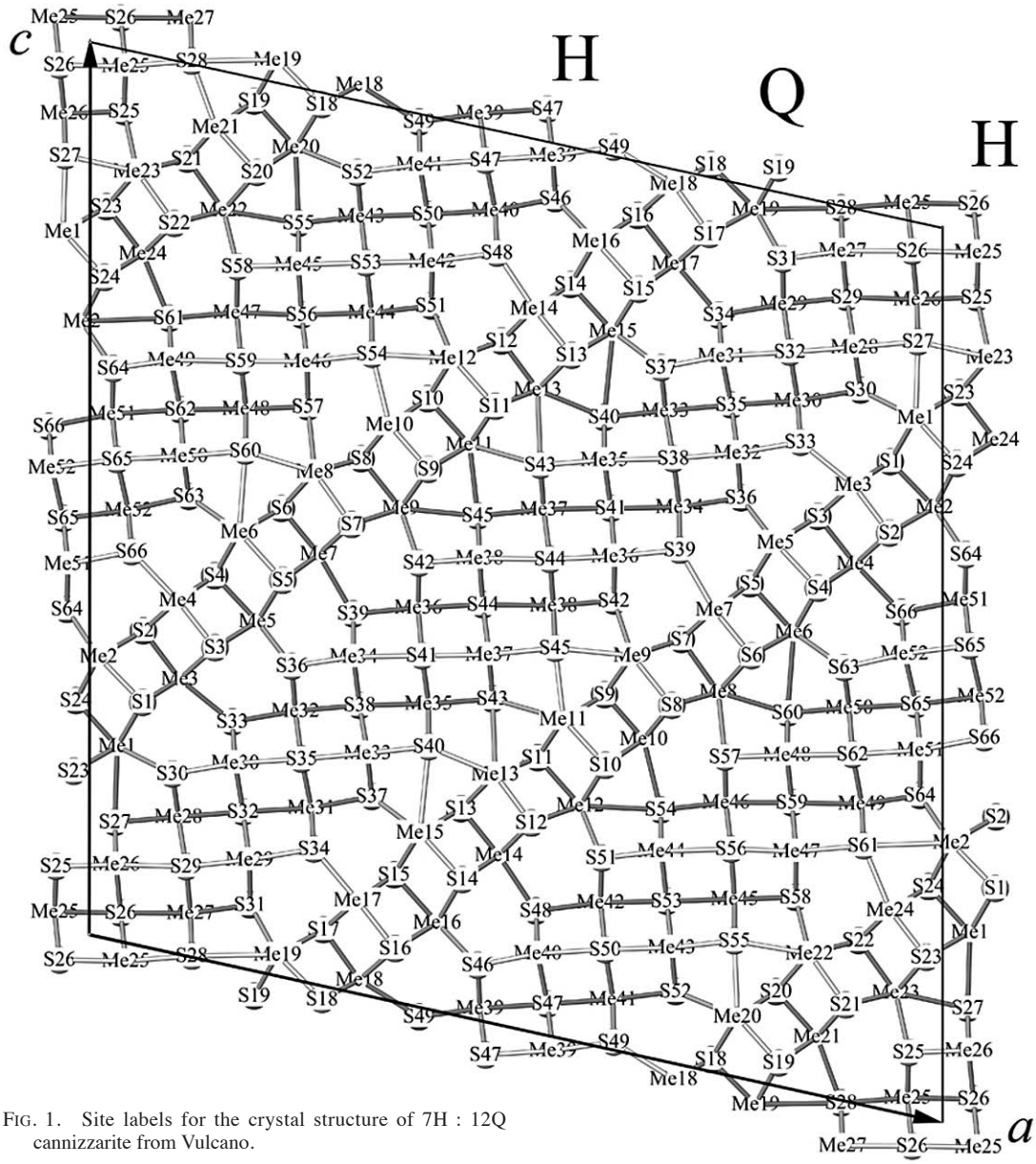

FIG. 1. Site labels for the crystal structure of 7H : 12Q cannizzarite from Vulcano.

the interlayer space and suggests a good accommodation of potential misfit problems. The positions *Me*3, 4, 7, 10, 14, 17, 18, 21 and 24 are predominantly Bi; *Me*1, 2, 5, 6, 8, 9, 12, 15, 16, 19, 22 and 23 are predominantly Pb. Inspection shows that almost all bismuth sites have the short in-plane distances too long for pure bismuth, and they plot close to the median line of the plot. The resulting configuration can be interpreted as the data points for Bi situated on a secant connecting two points of Bi hyperbola characterized by a combination of 2.70 and 3.00 Å distances in this and in the opposite order. The Bi positions are then unresolved split-cation positions in which two close, partly occupied Bi sites have the shorter *versus* longer distances in the base of the coordination pyramid oriented in the opposite way. Details of these procedures are in Berlepsch *et al*. (2001a, b) and Makovicky *et al*. (in prep.). Proximity of the in-plane data-point to the median line in Figure 3

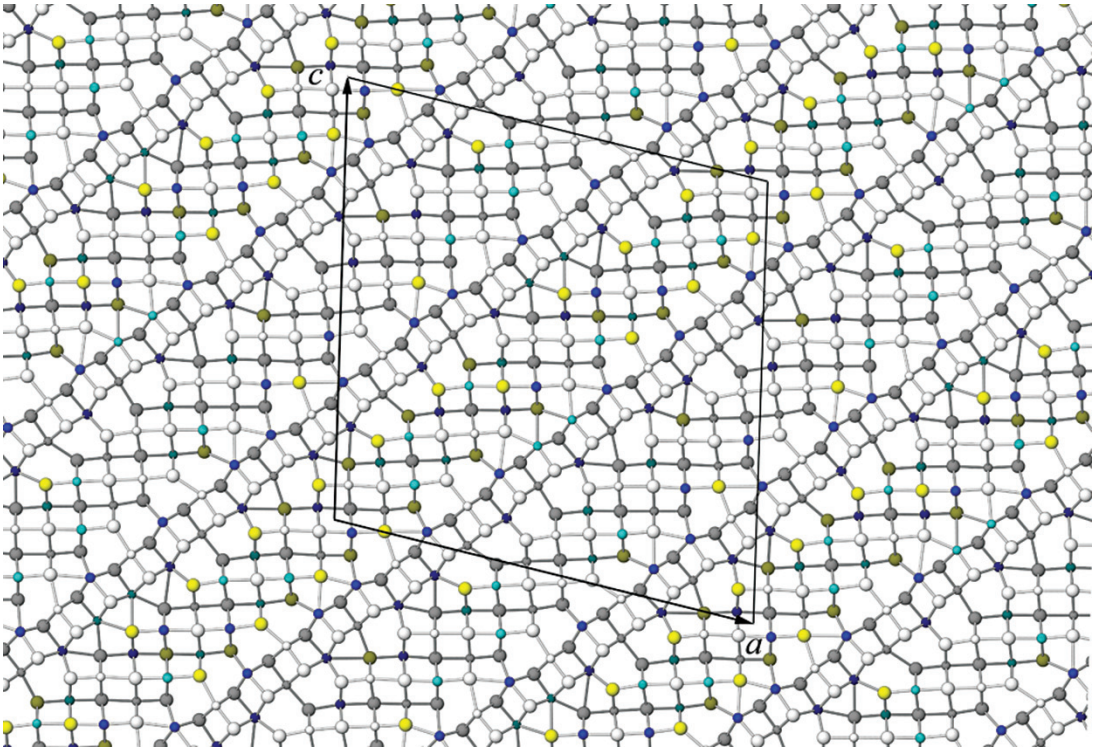

FIG. 2. The crystal structure of 7H : 12Q cannizzarite from Vulcano projected along the *b* direction (4.09 Å). The unit cell is shown. In the order of decreasing size, circles represent S and (S,Se), Pb (dark blue) and Bi sites. Light and dark spheres represent atoms at two *y* levels, ~2 Å apart. The anion sites with selenium are indicated by yellow circles, and the mixed (Bi,Pb) cation sites are indicated by cyan circles.

appears well correlated with the symmetry of the interlayer configuration of a given Bi site in Figure 1.

For *Me*39–*Me*52, the H layers exhibit imperfect pairing, especially of Bi–Bi, of cation polyhedra across the layer, and imperfect alternation of Pb (or of Pb–Pb pairs) with Bi or mixed sites along the modulated direction of the layer (Fig. 2). Similar instances of pairing and imperfect alternation of Pb and Bi (or mixed sites) are observed in the Q layer (Fig. 2). Any obvious correlation in site occupancies across the interlayer space appears to be absent, and the distribution of Bi sites in the Q layer follows primarily the distribution of octahedron configurations offered by the interlayer match.

The refined structure shows that the H component is sinusoidally modulated with a period of 3½ H subcells. It is much less transversally modulated than the Q component, which also appears to have the same modulation period (6 Q subcells long) superimposed on one or more short-wavelength modulations (or, perhaps even crenellations). Exact data on this modulation require superspace refinement. The H layer in the 12Q : 7H module of the cannizzarite structure refined by Matzat (1979b) displays the same sinusoidal modulation as the H layer in the present structure, whereas the pronounced crenellation of the Q layer in Matzat's

FIG. 3. Bond-length ratio hyperbolae (Trömmel 1981) of cations in the structure of cannizzarite, plotted in a way described in detail by Berlepsch *et al*. (2001a, b). The bond-length ratios of opposing *Me*–(S,Se) bonds are divided into the "in-plane" and "out-of-plane" sets. The former set describes the bonding situation in the base of the "square" coordination pyramid MeX_5, whereas the latter set combines the bond length to the vertex of the pyramid with an additional, long *Me*–S distance below the base. These two sets are plotted in the opposing sectors of the diagram, the in-plane set in the "upper", and the out-of-plane set in the "lower" sector, respectively, and are separated by the diagonal of the diagram, for which the opposing bonds have equal lengths. The hyperbola for Pb is taken from Berlepsch *et al*. (2001b), and that for Bi, from Topa *et al*. (2003). a) *Me* sites for the H layer; b) *Me* sites for the Q layer.

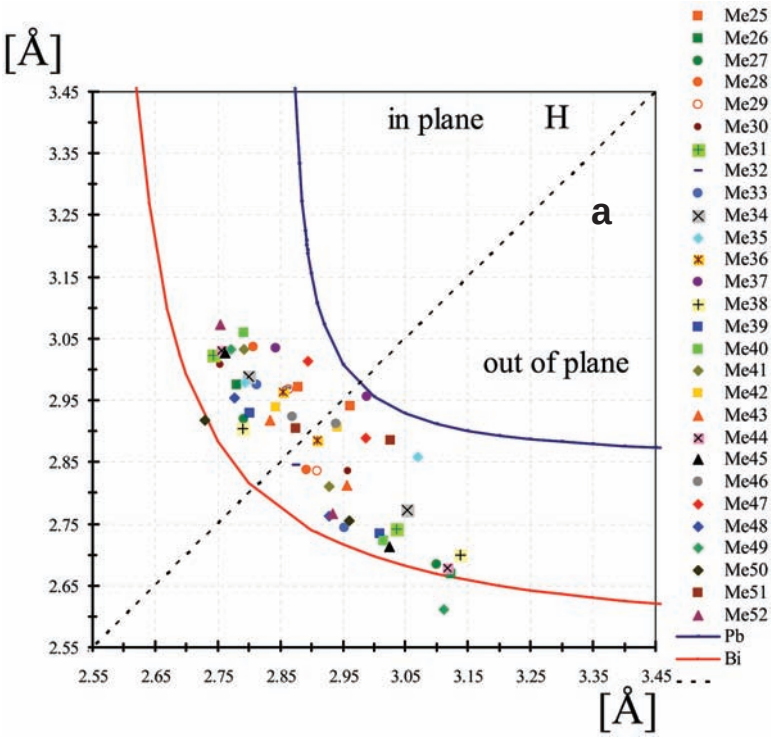
[Å]
in plane H
a
out of plane
3.45
3.35
3.25
3.15
3.05
2.95
2.85
2.75
2.65
2.55
2.55 2.65 2.75 2.85 2.95 3.05 3.15 3.25 3.35 3.45
[Å]
Me25
Me26
Me27
Me28
Me29
Me30
Me31
Me32
Me33
Me34
Me35
Me36
Me37
Me38
Me39
Me40
Me41
Me42
Me43
Me44
Me45
Me46
Me47
Me48
Me49
Me50
Me51
Me52
Pb
Bi

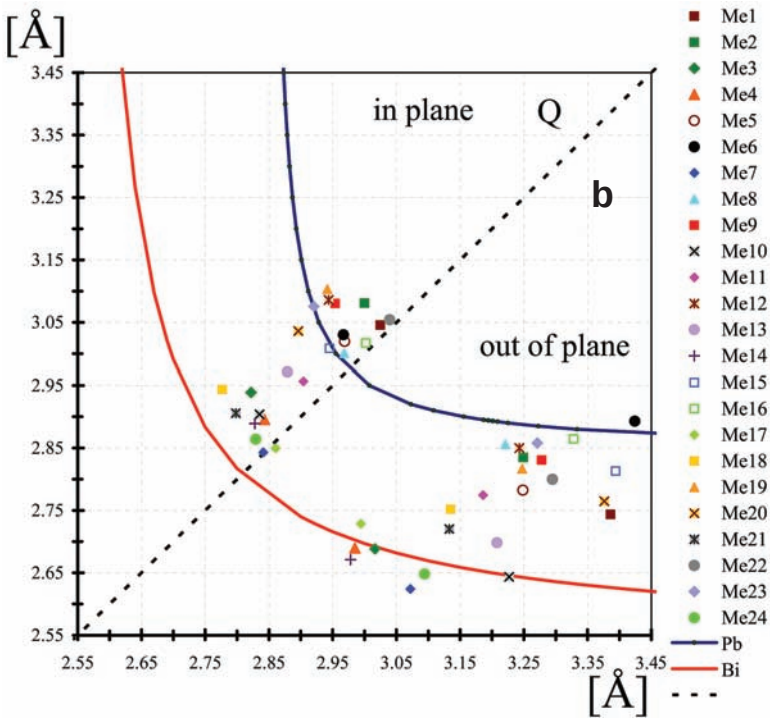
[Å]
in plane Q
b
out of plane
3.45
3.35
3.25
3.15
3.05
2.95
2.85
2.75
2.65
2.55
2.55 2.65 2.75 2.85 2.95 3.05 3.15 3.25 3.35 3.45
[Å]
Me1
Me2
Me3
Me4
Me5
Me6
Me7
Me8
Me9
Me10
Me11
Me12
Me13
Me14
Me15
Me16
Me17
Me18
Me19
Me20
Me21
Me22
Me23
Me24
Pb
Bi

TABLE 2. FINAL COORDINATES AND ANISOTROPIC DISPLACEMENT PARAMETERS OF ATOMS IN CANNIZZARITE FROM VULCANO

ATOM	*label*	*x*	*y*	*z*	sof	U_{eq}, U_{iso}	U_{11}	U_{22}	U_{33}	U_{13}
*Me*1	Pb	0.0318(1)	0.75	0.2191(1)		0.023(1)	0.018(2)	0.020(2)	0.027(3)	-0.002(2)
*Me*2	Pb	0.0098(1)	0.25	0.3147(1)		0.027(1)	0.042(3)	0.020(2)	0.016(3)	-0.001(2)
*Me*3	Bi	0.1050(1)	0.75	0.3093(1)		0.020(1)	0.021(2)	0.017(2)	0.020(3)	0.001(2)
*Me*4	Bi	0.1027(1)	0.25	0.3970(1)		0.020(1)	0.024(2)	0.027(2)	0.008(3)	0.001(2)
*Me*5	Pb	0.1962(1)	0.75	0.3929(1)		0.028(1)	0.033(2)	0.029(2)	0.024(3)	0.010(2)
*Me*6	Pb	0.1749(1)	0.25	0.4883(1)		0.030(1)	0.025(2)	0.032(3)	0.035(3)	0.012(2)
*Me*7	Bi	0.2681(1)	0.75	0.4830(1)		0.025(1)	0.017(2)	0.027(2)	0.030(3)	0.005(2)
*Me*8	Pb	0.2633(1)	0.25	0.5737(1)		0.031(1)	0.031(2)	0.028(3)	0.034(3)	0.004(2)
*Me*9	Pb	0.3643(1)	0.75	0.5541(1)		0.034(1)	0.046(3)	0.034(3)	0.019(3)	0.002(2)
*Me*10	Bi	0.3508(1)	0.25	0.6447(1)		0.030(1)	0.047(3)	0.023(2)	0.019(3)	0.004(2)
*Me*11	mixed	0.4450(1)	0.75	0.6420(1)		0.035(1)	0.043(3)	0.031(3)	0.026(3)	-0.002(2)
*Me*12	Pb	0.4252(1)	0.25	0.7344(1)		0.026(1)	0.026(2)	0.027(3)	0.018(2)	-0.011(2)
*Me*13	mixed	0.4751(1)	0.25	0.2800(1)		0.031(1)	0.027(2)	0.025(2)	0.033(3)	-0.011(2)
*Me*14	Bi	0.4793(1)	0.75	0.1903(1)		0.022(1)	0.023(2)	0.018(2)	0.026(3)	0.007(2)
*Me*15	Pb	0.3869(1)	0.25	0.1963(1)		0.026(1)	0.016(2)	0.024(2)	0.037(3)	0.002(2)
*Me*16	Pb	0.4070(1)	0.75	0.1001(1)		0.027(1)	0.031(2)	0.017(2)	0.031(3)	0.004(2)
*Me*17	Bi	0.3134(1)	0.25	0.1056(1)		0.020(1)	0.017(2)	0.013(2)	0.030(3)	0.003(2)
*Me*18	Bi	0.3158(1)	0.75	0.0172(1)		0.027(1)	0.030(2)	0.011(2)	0.037(3)	0.002(2)
*Me*19	Pb	0.2195(1)	0.25	0.0253(1)		0.028(1)	0.037(2)	0.019(2)	0.031(3)	0.014(2)
*Me*20	Pb	0.2410(1)	0.75	0.9318(1)		0.021(1)	0.015(2)	0.013(2)	0.033(3)	-0.001(2)
*Me*21	Bi	0.1474(1)	0.25	0.9349(1)		0.019(1)	0.020(2)	0.010(2)	0.027(3)	0.005(2)
*Me*22	Pb	0.1566(1)	0.75	0.8439(1)		0.027(1)	0.028(2)	0.016(2)	0.035(3)	0.001(2)
*Me*23	Pb	0.0550(1)	0.25	0.8664(1)		0.023(1)	0.032(2)	0.017(2)	0.015(3)	-0.010(2)
*Me*24	Bi	0.0617(1)	0.75	0.7755(1)		0.020(1)	0.020(2)	0.019(2)	0.018(3)	-0.002(2)
*Me*25	Pb	0.0415(1)	0.25	0.9811(1)		0.014(1)	0.011(2)	0.006(2)	0.021(3)	-0.007(2)
*Me*26	Bi	0.0304(1)	0.25	0.0867(1)		0.014(1)	0.010(2)	0.012(2)	0.015(3)	-0.007(2)
*Me*27	Bi	0.1176(1)	0.75	0.0504(1)		0.014(1)	0.013(2)	0.006(2)	0.018(3)	-0.008(2)
*Me*28	mixed	0.1036(1)	0.75	0.1552(1)		0.018(1)	0.016(2)	0.007(2)	0.025(3)	-0.011(2)
*Me*29	mixed	0.1869(1)	0.25	0.1244(1)		0.015(1)	0.016(2)	0.008(2)	0.019(3)	-0.001(2)
*Me*30	mixed	0.1701(1)	0.25	0.2290(1)		0.020(1)	0.016(2)	0.011(2)	0.029(3)	-0.004(2)
*Me*31	mixed	0.2593(1)	0.75	0.1974(1)		0.016(1)	0.021(2)	0.008(2)	0.016(3)	-0.002(2)
*Me*32	Pb	0.2406(1)	0.75	0.3019(1)		0.017(1)	0.012(2)	0.016(2)	0.018(3)	-0.004(2)
*Me*33	Bi	0.3253(1)	0.25	0.2724(1)		0.017(1)	0.011(2)	0.011(2)	0.024(3)	-0.005(2)
*Me*34	mixed	0.3089(1)	0.25	0.3767(1)		0.014(1)	0.005(2)	0.019(2)	0.013(3)	-0.008(2)
*Me*35	Pb	0.3969(1)	0.75	0.3424(1)		0.016(1)	0.009(2)	0.019(2)	0.015(3)	-0.006(2)
*Me*36	mixed	0.3847(1)	0.75	0.4474(1)		0.016(1)	0.019(2)	0.022(2)	0.005(3)	0.002(2)
*Me*37	Pb	0.4679(1)	0.25	0.4122(1)		0.019(1)	0.015(2)	0.016(2)	0.021(3)	-0.007(2)
*Me*38	Bi	0.4567(1)	0.25	0.5173(1)		0.017(1)	0.013(2)	0.028(2)	0.006(3)	-0.006(2)
*Me*39	Bi	0.4572(1)	0.75	0.0147(1)		0.020(1)	0.022(2)	0.015(2)	0.022(3)	0.006(2)
*Me*40	Bi	0.4751(1)	0.75	0.9101(1)		0.024(1)	0.029(2)	0.015(2)	0.025(3)	0.001(2)
*Me*41	mixed	0.3868(1)	0.25	0.9428(1)		0.021(1)	0.025(2)	0.017(2)	0.024(3)	0.008(2)
*Me*42	mixed	0.4012(1)	0.25	0.8375(1)		0.023(1)	0.024(2)	0.018(2)	0.026(3)	-0.001(2)
*Me*43	mixed	0.3180(1)	0.75	0.8708(1)		0.019(1)	0.025(2)	0.019(2)	0.015(3)	0.009(2)
*Me*44	Bi	0.3301(1)	0.75	0.7655(1)		0.022(1)	0.027(2)	0.016(2)	0.024(3)	0.009(2)
*Me*45	Bi	0.2443(1)	0.25	0.8012(1)		0.020(1)	0.020(2)	0.019(2)	0.027(3)	0.005(2)
*Me*46	mixed	0.2545(1)	0.25	0.6940(1)		0.024(1)	0.032(2)	0.028(3)	0.014(3)	0.007(2)
*Me*47	Pb	0.1720(1)	0.75	0.7329(1)		0.028(1)	0.024(2)	0.028(3)	0.031(3)	0.001(2)
*Me*48	Bi	0.1827(1)	0.75	0.6275(1)		0.027(1)	0.025(2)	0.031(3)	0.027(3)	0.006(2)
*Me*49	Bi	0.0951(1)	0.25	0.6638(1)		0.030(1)	0.031(2)	0.028(3)	0.037(3)	0.016(2)
*Me*50	Bi	0.1098(1)	0.25	0.5594(1)		0.024(1)	0.026(2)	0.038(3)	0.013(3)	0.013(2)
*Me*51	Pb	0.0261(1)	0.75	0.5893(1)		0.032(1)	0.030(2)	0.039(3)	0.027(3)	0.009(2)
*Me*52	Bi	0.0448(1)	0.75	0.4855(1)		0.032(1)	0.033(2)	0.042(3)	0.024(3)	0.012(2)
S1	S	0.0616(9)	0.25	0.2743(9)		0.041(8)				
S2	S	0.0624(6)	0.75	0.3544(6)		0.013(5)				
S3	S	0.1465(6)	0.25	0.3532(7)		0.017(5)				
S4	S	0.1460(5)	0.75	0.4334(6)		0.000(6)				
S5	S	0.2260(6)	0.25	0.4450(7)		0.019(6)				
S6	S	0.2243(7)	0.75	0.5250(7)		0.020(6)				
S7	S	0.3067(7)	0.25	0.5241(7)		0.021(6)				
S8	S	0.3178(5)	0.75	0.5999(6)		0.008(5)				
S9	S	0.3969(6)	0.25	0.6044(6)		0.013(5)				
S10	S	0.3958(6)	0.75	0.6831(6)		0.015(5)				
S11	S	0.4751(8)	0.25	0.6912(8)		0.036(8)				

TABLE 2 (cont'd). FINAL COORDINATES AND ANISOTROPIC DISPLACEMENT PARAMETERS OF ATOMS IN CANNIZZARITE FROM VULCANO

ATOM	*label*	*x*	*y*	*z*	sof	U_{eq}, U_{iso}	U_{11}	U_{22}	U_{33}	U_{13}
S12	S	0.5175(5)	0.25	0.2343(6)		0.009(4)				
S13	S	0.4351(5)	0.75	0.2332(6)		0.004(4)				
S14	S	0.4365(6)	0.25	0.1543(7)		0.018(5)				
S15	S	0.3564(6)	0.75	0.1430(7)		0.015(5)				
S16	S	0.3578(5)	0.25	0.0608(6)		0.008(5)				
S17	S	0.2736(6)	0.75	0.0645(6)		0.013(5)				
S18	S	0.2720(7)	0.25	0.9862(7)		0.023(6)				
S19	S	0.1924(6)	0.75	0.9734(7)		0.000(7)				
S20	S	0.1956(5)	0.25	0.8945(5)		0.000(4)				
S21	S	0.1138(6)	0.75	0.8923(6)		0.014(5)				
S22	S	0.0988(7)	0.25	0.8173(7)		0.020(6)				
S23	S	0.0192(5)	0.75	0.8194(6)		0.002(6)				
S24	S	0.9833(7)	0.75	0.2601(7)		0.020(6)				
(**S**,Se)25	mixed	0.0398(4)	0.75	0.9300(5)	0.57(6)/0.43(6)	0.024(5)				
S26	S	0.0359(7)	0.75	0.0338(7)		0.020(5)				
(**S**,Se)27	mixed	0.0291(5)	0.75	0.1336(5)	0.86(6)/0.14(6)	0.014(6)				
(**S**,Se)28	mixed	0.1193(5)	0.25	1.0029(5)	0.69(6)/0.31(6)	0.020(6)				
S29	S	0.1126(5)	0.25	0.1014(6)		0.008(4)				
(**S**,Se)30	mixed	0.0965(4)	0.25	0.2016(5)	0.62(4)/0.38(6)	0.022(5)				
(**S**,Se)31	mixed	0.1876(6)	0.75	0.0742(6)	0.77(6)/0.23(6)	0.027(7)				
S32	S	0.1793(6)	0.75	0.1765(6)		0.013(5)				
(**S**,Se)33	mixed	0.1668(5)	0.75	0.2745(6)	0.90(6)/0.10(6)	0.016(6)				
S34	S	0.2624(6)	0.25	0.1523(6)		0.012(5)				
S35	S	0.2479(5)	0.25	0.2497(6)		0.005(4)				
(**S**,Se)36	mixed	0.2367(5)	0.25	0.3512(5)	0.73(6)/0.27(6)	0.023(6)				
(**S**,Se)37	mixed	0.3303(5)	0.75	0.2251(5)	0.67(6)/0.33(6)	0.025(6)				
S38	S	0.3160(5)	0.75	0.3239(6)		0.008(4)				
(**S**,Se)39	mixed	0.3085(5)	0.75	0.4246(6)	0.76(6)/0.24(6)	0.025(7)				
S40	S	0.3971(5)	0.25	0.2946(5)		0.001(4)				
(**S**,Se)41	mixed	0.3893(6)	0.25	0.3946(6)	0.89(6)/0.11(6)	0.021(7)				
S42	S	0.3858(5)	0.25	0.4976(6)		0.006(4)				
(S,**Se**)43	mixed	0.4719(4)	0.75	0.3637(4)	0.44(6)/0.56(6)	0.031(5)				
S44	S	0.4606(6)	0.75	0.4665(6)		0.007(6)				
S45	S	0.4546(6)	0.75	0.5645(7)		0.015(5)				
S46	S	0.4546(5)	0.25	0.0622(6)		0.003(4)				
S47	S	0.4637(7)	0.25	0.9639(7)		0.022(6)				
S48	S	0.4772(7)	0.25	0.8628(7)		0.023(6)				
S49	S	0.3859(5)	0.75	0.9904(6)		0.009(4)				
S50	S	0.3960(8)	0.75	0.8891(8)		0.031(7)				
S51	S	0.4001(6)	0.75	0.7877(6)		0.009(5)				
(**S**,Se)52	mixed	0.3134(4)	0.25	0.9189(5)	0.82(6)/0.18(6)	0.012(5)				
S53	S	0.3238(7)	0.25	0.8201(8)		0.029(7)				
S54	S	0.3307(5)	0.25	0.7193(6)		0.007(4)				
S55	S	0.2444(5)	0.75	0.8478(6)		0.004(4)				
S56	S	0.2481(6)	0.75	0.7461(7)		0.019(6)				
S57	S	0.2554(5)	0.75	0.6449(6)		0.004(4)				
S58	S	0.1728(8)	0.25	0.7844(8)		0.031(7)				
S59	S	0.1770(7)	0.25	0.6795(8)		0.026(6)				
(**S**,Se)60	mixed	0.1820(6)	0.25	0.5802(6)	0.78(6)/0.22(6)	0.034(8)				
(**S**,Se)61	mixed	0.0928(5)	0.75	0.7101(6)	0.89(6)/0.11(6)	0.015(7)				
S62	S	0.1058(9)	0.75	0.6107(9)		0.041(8)				
S63	S	0.1157(6)	0.75	0.5157(7)		0.015(5)				
S64	S	0.0271(8)	0.25	0.6402(8)		0.035(8)				
S65	S	0.0315(9)	0.25	0.5394(9)		0.057(9)				
S66	S	0.0485(7)	0.25	0.4401(8)		0.026(6)				

U_{12} = 0, U_{13} = 0 by symmetry, *Me*1–*Me*24 are positioned in the Q layers, whereas *Me*25–*Me*52 belong to the H layers.

structure refinement prevents closer comparison with our results.

Conclusions

The present refinement of the crystal structure of cannizzarite confirms the independent existence of one of the component modules of the complex structure originally proposed of by Matzat (1979a, b) and gives credence to the hypothesis that the composition and crystallography of natural cannizzarite might lie between the end-members $Pb_{12}Bi_{14}S_{33}$ and $Pb_{17}Bi_{20}S_{47}$ (with a potential for partial Se-for-S substitution). Thus, "cannizzarite" is a narrow, *variable-fit homologous series* (Makovicky 1988) of structures and compositions and not a single phase, as already suggested by Makovicky & Hyde (1981).

There are at least two ways of explaining the *chemical variations* reported for cannizzarite in the literature quoted. As mentioned above, cannizzarite is a variable-fit homologous series in which the change in the values of *m* and *n* in the formula *m*Q: *n*H that expresses the

TABLE 3. SELECTED INTERATOMIC DISTANCES (Å) IN CANNIZZARITE FROM VULCANO

*Me*1–	*Me*2–	*Me*3–	*Me*4–	*Me*5–	*Me*6–	*Me*7–
S24 2.743(29)	S1 2.831(39)	S2 2.690(27)	S3 2.687(29)	S4 2.784(29)	S5 2.894(29)	S6 2.625(31)
S23 3.027(14) ×2	S24 3.002(19) ×2	S1 2.823(22) ×2	S4 2.843(13) ×2	S5 2.967(18) ×2	S6 2.966(18) ×2	S7 2.841(17) ×2
S1 3.046(25) ×2	S2 3.080(16) ×2	S3 2.940(17) ×2	S2 2.895(15) ×2	S3 3.019(17) ×2	S4 3.030(16) ×2	S5 2.844(16) ×2
S27 3.385(21)	S64 3.252(27) ×2	S33 3.018(24)	S66 2.985(33)	S36 3.245(17) ×2	S63 3.427(21) ×2	S39 3.072(22)
S30 3.428(14) ×2	S61 3.899(20)				S60 3.611(25)	
*Me*8–	*Me*9–	*Me*10–	*Me*11–	*Me*12–	*Me*13–	*Me*14–
S7 2.858(31)	S8 2.828(25)	S9 2.643(27)	S10 2.774(29)	S11 2.855(35)	S12 2.699(25)	S13 2.669(25)
S8 2.969(14) ×2	S9 2.953(16) ×2	S8 2.835(15) ×2	S11 2.900(21) ×2	S10 2.944(18) ×2	S11 2.882(20) ×2	S14 2.827(16) ×2
S6 3.001(18) ×2	S7 3.079(19) ×2	S10 2.903(16) ×2	S9 2.957(16) ×2	S12 3.086(14) ×2	S13 2.971(15) ×2	S12 2.889(14) ×2
S60 3.226(25)	S42 3.281(20) ×2	S54 3.232(25)	S45 3.187(29)	S51 3.244(20) ×2	S40 3.209(21)	S48 2.976(31)
S57 3.562(18) ×2	S45 3.446(24)		S43 3.868(15) ×2	S54 3.592(20)	S43 3.936(15) ×2	
*Me*15–	*Me*16–	*Me*17–	*Me*18–	*Me*19–	*Me*20–	*Me*21–
S14 2.810(29)	S15 2.867(29)	S16 2.732(25)	S17 2.751(27)	S18 2.818(31)	S19 2.768(28)	S20 2.718(22)
S13 2.946(14) ×2	S16 3.001(14) ×2	S15 2.852(16) ×2	S18 2.776(17) ×2	S19 2.940(18) ×2	S20 2.896(13) ×2	S21 2.797(15) ×2
S15 3.005(19) ×2	S14 3.018(19) ×2	S17 2.859(15) ×2	S16 2.943(14) ×2	S17 3.105(16) ×2	S18 3.036(19) ×2	S19 2.905(16) ×2
S37 3.377(17) ×2	S46 3.328(19) ×2	S34 2.996(26)	S49 3.130(23)	S31 3.247(20) ×2	S55 3.377(25)	S28 3.128(21)
		S40 3.849(21)		S28 3.807(16)	S52 3.604(15) ×2	
*Me*22–	*Me*23–	*Me*24–	*Me*25–	*Me*26–	*Me*27–	*Me*28–
S21 2.802(27)	S22 2.852(31)	S23 2.649(25)	S25 2.876(12) ×2	S25 2.668(16)	S31 2.685(19)	S30 2.808(12) ×2
S20 3.041(14) ×2	S23 2.918(15) ×2	S22 2.830(17) ×2	S26 2.941(27)	S27 2.779(14) ×2	S28 2.796(14) ×2	S27 2.839(19)
S22 3.055(19) ×2	S21 3.076(17) ×2	S24 2.863(16) ×2	S28 2.962(16)	S26 2.975(21) ×2	S29 2.918(18) ×2	S32 2.885(23)
S58 3.290(27) ×2	S27 3.270(21)	S61 3.097(25)	S26 2.972(21) ×2	S29 3.123(20)	S26 3.102(27)	S29 3.037(19) ×2
	S55 3.384(21)	S25 3.405(14) ×2				
*Me*29–	*Me*30–	*Me*31–	*Me*32–	*Me*33–	*Me*34–	*Me*35–
S29 2.838(19)	S33 2.753(17) ×2	S34 2.741(17) ×2	S33 2.844(19)	S40 2.741(19)	S36 2.774(19)	S40 2.794(14) ×2
S31 2.863(17) ×2	S30 2.838(15)	S37 2.744(19)	S36 2.862(15) ×2	S37 2.814(15) ×2	S39 2.799(14) ×2	S43 2.858(15)
S34 2.909(21)	S35 2.959(19)	S35 3.019(19) ×2	S38 2.874(19)	S35 2.952(19)	S38 2.988(18) ×2	S41 2.977(19) ×2
S32 2.974(19) ×2	S32 3.000(19) ×2	S32 3.045(23)	S35 2.973(18) ×2	S38 2.974(18) ×2	S41 3.053(23)	S38 3.072(19)
*Me*36–	*Me*37–	*Me*38–	*Me*39–	*Me*40–	*Me*41–	*Me*42–
S42 2.853(17) ×2	S43 2.843(12) ×2	S42 2.701(19)	S49 2.735(19)	S46 2.721(19)	S49 2.794(17) ×2	S51 2.844(17) ×2
S44 2.886(23)	S45 2.956(23)	S45 2.790(20) ×2	S46 2.803(17) ×2	S48 2.793(20) ×2	S52 2.808(15)	S48 2.910(26)
S39 2.907(19)	S41 2.987(23)	S44 2.904(18) ×2	S47 2.925(21) ×2	S50 3.009(27)	S47 2.928(27)	S50 2.936(24) ×2
S41 2.965(18) ×2	S44 3.033(19) ×2	S44 3.140(23)	S47 3.009(27)	S47 3.063(22) ×2	S50 3.035(25) ×2	S53 2.941(27)
*Me*43–	*Me*44–	*Me*45–	*Me*46–	*Me*47–	*Me*48–	*Me*49–
S55 2.812(19)	S51 2.676(19)	S58 2.715(31)	S57 2.874(17) ×2	S58 2.892(23) ×2	S57 2.764(19)	S64 2.609(30)
S52 2.835(15) ×2	S54 2.754(17) ×2	S55 2.760(17) ×2	S54 2.913(19)	S56 2.894(23)	S60 2.777(17) ×2	S61 2.769(17) ×2
S53 2.915(24) ×2	S53 3.033(25) ×2	S53 3.023(27)	S56 2.922(21) ×2	S59 2.987(24) ×2	S62 2.920(34)	S62 3.033(26) ×2
S50 2.964(27)	S56 3.116(23)	S56 3.027(21) ×2	S59 2.942(27)	S61 3.017(19)	S59 2.952(24) ×2	S59 3.112(27)
*Me*50–	*Me*51–	*Me*52–				
S63 2.728(17) ×2	S64 2.873(23) ×2	S66 2.754(22) ×2				
S60 2.753(23)	S66 2.887(26)	S63 2.761(22)				
S62 2.917(24) ×2	S65 2.892(30) ×2	S65 2.921(41)				
S65 2.976(42)	S62 3.033(34)	S65 3.088(32) ×2				

TABLE 4. POLYHEDRON CHARACTERISTICS FOR METAL ATOMS IN THE STRUCTURE OF CANNIZZARITE FROM VULCANO

1	1a	2	3	4	5	6	7	8	9
*Me*1	Pb	8	3.136	0.029	0.332	0.999	129.135	54.357	1.96
*Me*2	Pb	8	3.167	0.041	0.352	0.814	133.077	55.347	1.86
*Me*3	Bi	6	2.878	0.026	0.170	0.975	99.874	30.976	2.62
*Me*4	Bi	6	2.865	0.013	0.148	0.976	98.472	30.948	2.69
*Me*5	Pb	7	3.047	0.122	0.237	0.999	118.451	39.349	2.05
*Me*6	Pb	8	3.161	0.042	0.332	0.900	132.304	54.920	1.84
*Me*7	Bi	6	2.856	0.021	0.217	0.995	97.597	30.427	2.88
*Me*8	Pb	8	3.200	0.027	0.394	0.779	137.217	65.302	2.03
*Me*9	Pb	8	3.113	0.034	0.271	0.926	126.422	52.956	1.99
*Me*10	Bi	6	3.085	0.183	0.482	0.708	123.014	38.042	2.70
*Me*11	m	8	3.164	0.044	0.484	0.793	132.715	55.027	2.22
*Me*12	Pb	8	3.127	0.038	0.276	0.876	128.034	53.386	1.96
*Me*13	m	8	3.169	0.046	0.521	0.776	133.299	55.139	2.34
*Me*14	Bi	6	2.857	0.019	0.158	0.974	97.640	30.505	2.79
*Me*15	Pb	8	3.151	0.045	0.392	0.837	130.987	54.240	2.01
*Me*16	Pb	7	3.094	0.121	0.248	0.971	124.032	41.268	1.82
*Me*17	Bi	6	2.864	0.008	0.132	1.000	98.352	31.068	2.66
*Me*18	Bi	6	2.893	0.059	0.206	0.974	101.448	30.388	2.57
*Me*19	Pb	8	3.147	0.039	0.335	0.820	130.597	54.391	1.97
*Me*20	Pb	8	3.141	0.032	0.421	0.933	129.832	54.505	2.10
*Me*21	Bi	6	2.888	0.056	0.208	0.978	100.847	30.310	2.64
*Me*22	Pb	8	3.118	0.030	0.259	0.966	126.952	53.383	1.92
*Me*23	Pb	8	3.116	0.033	0.304	0.967	126.731	53.110	2.01
*Me*24	Bi	6	2.873	0.043	0.218	0.999	99.305	30.254	2.79
*Me*25	Pb	6	2.932	0.003	0.069	0.987	105.625	33.518	2.14
*Me*26	Bi	6	2.883	0.005	0.247	0.991	100.426	31.806	2.65
*Me*27	Bi	6	2.869	0.004	0.219	0.985	98.965	31.373	2.69
*Me*28	m	6	2.902	0.004	0.159	0.971	102.367	32.461	2.40
*Me*29	m	6	2.903	0.005	0.083	0.975	102.525	32.474	2.33
*Me*30	m	6	2.880	0.000	0.182	0.989	100.047	31.838	2.54
*Me*31	m	6	2.878	0.000	0.236	0.992	99.879	31.784	2.61
*Me*32	Pb	6	2.896	0.001	0.080	0.968	101.787	32.371	2.37
*Me*33	Bi	6	2.877	0.001	0.151	0.976	99.793	31.724	2.55
*Me*34	m	6	2.896	0.000	0.188	0.990	101.703	32.362	2.44
*Me*35	Pb	6	2.909	0.001	0.161	0.956	103.090	32.789	2.34
*Me*36	m	6	2.904	0.002	0.080	0.993	102.587	32.579	2.32
*Me*37	Pb	6	2.947	0.002	0.129	0.983	107.245	34.078	2.09
*Me*38	Bi	6	2.875	0.006	0.226	0.965	99.498	31.488	2.68
*Me*39	Bi	6	2.866	0.001	0.162	0.996	98.575	31.347	2.63
*Me*40	Bi	6	2.900	0.000	0.227	0.967	102.153	32.505	2.46
*Me*41	m	6	2.896	0.002	0.176	0.978	101.734	32.336	2.43
*Me*42	m	6	2.900	0.003	0.068	0.982	102.160	32.439	2.33
*Me*43	m	6	2.879	0.001	0.095	0.994	99.936	31.774	2.49
*Me*44	Bi	6	2.892	0.002	0.277	0.999	101.353	32.189	2.62
*Me*45	Bi	6	2.886	0.003	0.234	0.991	100.663	31.942	2.60
*Me*46	m	6	2.907	0.002	0.037	0.985	102.868	32.676	2.29
*Me*47	Pb	6	2.945	0.005	0.091	0.995	107.024	33.908	2.09
*Me*48	Bi	6	2.855	0.001	0.147	0.990	97.480	30.988	2.69
*Me*49	Bi	6	2.881	0.004	0.284	0.976	100.199	31.781	2.72
*Me*50	Bi	6	2.838	0.006	0.173	0.978	95.776	30.318	2.87
*Me*51	Pb	6	2.906	0.006	0.077	0.958	102.814	32.536	2.30
*Me*52	Bi	6	2.888	0.002	0.239	0.960	100.917	32.076	2.55

1) Metal site, 1a) site label; m denotes a mixed site, 2) coordination number, 3) radius r_s of a circumscribed sphere, least-squares fitted to the coordination polyhedron, 4) "volume-based" distortion $u = [V(\text{ideal polyhedron}) - V(\text{real polyhedron})] / V(\text{ideal polyhedron})$; the ideal polyhedron has the same number of ligands, 5) "volume-based" eccentricity $ECC_v = 1 - [(r_s - \Delta)/r_s]^3$; Δ is the distance between the center of the sphere and the central atom in the polyhedron, 6) "volume-based" sphericity $SPH_v = 1 - 3\sigma_r r_s$; σ_r is a standard deviation of the radius r_s, 7) volume of the circumscribed sphere, 8) volume of coordination polyhedron, 9) bond-valence sum.

number of matching subcells means automatically a change in the Pb:Bi and cation:anion ratio. It should be noted, however, that the difference between the compositions of the two (potentially) limiting modules lies within the error bounds of electron-microprobe analysis. The other possibility is the occurrence of H or Q layers with a wrong thickness (thinner or thicker ones than in the periodic structure of cannizzarite) or an occasional lack of (especially) Q layer between two adjacent H layers. Model calculations for these mecha-

nisms are in Makovicky & Hyde (1992). The presence of cation vacancies assumed by Mozgova *et al*. (1992) is considered unlikely; the relatively thin layers will probably collapse and form another structure because the large empty polyhedra with uncompensated anions will be unstable. This might precisely be the way to change from cannizzarite to the closely related but more complicated structure of weibullite (Mumme 1980).

Selenium shows a strong preference for the marginal anion sites of the H layer, as was also observed by Mumme (1980) for weibullite, Mumme (1976) and Mumme *et al*. (2009) for proudite, and suggested by Mozgova *et al*. (1992) for cannizzarite. The latter authors based their explanation on the analogy of the H layers in cannizzarite and those in the tetradymite series. Our explanation, mentioned briefly in Mumme *et al*. (2009) for proudite, is based on the difference between the bonds connecting the cations and the central anions of the H layer, and those connecting the cations and the marginal anions of this layer, *i.e*., on the bonding scheme of, especially, bismuth in the H layer. The former distances are appreciably longer than the latter, and the resulting problems in constructing a coherent two-octahedron layer will be greatly alleviated if a mechanism is found to make the latter distances longer, in this case by replacing S^{2-}, with a radius in sulfide crystals equal to 1.70 Å, by Se^{2-}, with a radius of 1.84 Å (Shannon 1981). The generally low Se contents in our H layers and the existence of selenium-free cannizzarite (Nowacki & Stalder 1969, Berlepsch *et al*. 2001, Topa *et al*. 2001) show, however, that these problems can be overcome without incorporation of selenium. Still, Mozgova *et al*. (1992) demonstrated that cannizzarite is selectively enriched in Se in comparison to the sulfides associated with it in the deposits of Nevskoye and Vulcano, *i.e*., the mechanism proposed is structurally preferred. It can be assumed that the selective incorporation of selenium in the H layers will also influence the *m*Q : *n*H match and, as a consequence, the Pb:Bi ratio, but in the absence of crystal-structure determinations on the Se-free cannizzarite, and absence of positional parameters for $Pb_5Bi_6Se_{14}$ in the publication of Zhang *et al*. (2005), this assumption cannot be verified.

Acknowledgments

The authors gratefully acknowledge the support of the Christian Doppler Research Society (Austria). EM was supported by the grant no.272-08-0227 of the Research Council for Nature and Universe (Denmark). We thank Drs. Yves Moëlo and Daniela Pinto for constructive reviews, and Prof. R.F. Martin for thoughtful review and editorial assistance.

References

Balić-Žunić, T. & Vicković, I. (1996): IVTON – a program for the calculation of geometrical aspects of crystal structures and some crystal chemical applications. *J. Appl. Crystallogr.* **29**, 305-306.

Berlepsch, P., Armbruster, T., Makovicky, E., Hejny, C., Topa, D. & Graeser, S. (2001): The crystal structure of (001) twinned xilingolite, $Pb_3Bi_2S_6$, from Mittal–Hohtenn, Valais, Switzerland. *Can. Mineral.* **39**, 1653-1663.

Berlepsch, P., Makovicky, E. & Balić-Žunić, T. (2001a): Crystal chemistry of sartorite homologues and related sulfosalts. *Neues Jahrb. Mineral., Monatsh.*, 45-66.

Berlepsch, P., Makovicky, E. & Balić-Žunić, T. (2001b): Crystal chemistry of meneghinite homologues and related sulfosalts. *Neues Jahrb. Mineral., Monatsh.*, 115-135.

Borodaev, Yu.S., Garavelli, A., Garbarino, C., Grillo, S.M., Mozgova, N.N., Organova, N.I. & Trubkin, N.V. (2000): Rare sulfosalts from Vulcano, Aeolian Islands, Italy. III. Wittite and cannizzarite. *Can. Mineral.* **38**, 23-34.

Bruker AXS (1997): Shelxtl, Version 5.1. Bruker AXS, Inc., Madison,Wisconsin 53719, U.S.A.

Bruker AXS (1998a): Smart, Version 5.0. Bruker AXS, Inc., Madison, Wisconsin 53719, U.S.A.

Bruker AXS (1998b): Saint, Version 5.0. Bruker AXS, Inc., Madison,Wisconsin 53719, U.S.A.

Ferraris, G., Makovicky, E. & Merlino, S. (2004): *Crystallography of Modular Materials*. Oxford University Press, Oxford, U.K.

Graham, A.R., Thompson, R.M. & Berry, L.G. (1953): Studies of mineral sulpho-salts. XVII. Cannizzarite. *Am. Mineral.* **38**, 536-544.

Makovicky, E. (1988): Classification of homologous series. *Z. Kristallogr.* **185**, 512.

Makovicky, E. & Hyde, B.G. (1981): Non-commensurate (misfit) layer structures. *Structure and Bonding* **46**, 101-170.

Makovicky, E. & Hyde, B.G. (1992): Incommensurate, two-layer structures with complex crystal chemistry: minerals and related synthetics. *Materials Sci. Forum* **100–101**, 1-100.

Makovicky, E., Petříček, V., Dušek, M. & Topa, D. (2008): Crystal structure of a synthetic tin–selenium representative of the cylindrite structure type. *Am. Mineral.* **93**, 1787-1798.

Matzat, E. (1979a): Cannizzarite. *Acta Crystallogr.* **B35**, 133-136.

Matzat, E. (1979b): *Strukturanalyse von Cannizzarit. Ein Beitrag zur Theorie modulierter Strukturen mit inkommensurablen Gittern*. Habilitationsschrift, Mathematisch-Naturwissenschaftliche Fakultät, Universität Göttingen, Göttingen, Germany.

MOËLO, Y., MAKOVICKY, E., MOZGOVA, N.N., JAMBOR, J.L., COOK, N., PRING, A., PAAR, W., NICKEL, E.H., GRAESER, S., KARUP-MØLLER, S., BALIĆ-ŽUNIĆ, T., MUMME, W.G., VURRO, F., TOPA, D., BINDI, L., BENTE, K. & SHIMIZU, M. (2008): Sulfosalt systematics: a review. Report of the sulfosalt sub-committee of the IMA Commission on Ore Mineralogy. *Eur. J. Mineral.* **20**, 7-46.

MOZGOVA, N.N., MOËLO, Y., BORODAEV, YU.S., NENASHEVA, S.N. & EFIMOV, A.V. (1992): Wittite with Se-rich cosalite and bismuthinite from Nevskoye tin deposit (Magadan District, Russia). *Mineral. Petrol.* **46**, 137-153.

MOZGOVA, N.N., ORGANOVA, N.I., BORODAEV, YU.S., RYBAYEVA, E.G., SIVTSOV, A.V., GETMANSKAYA, O.V. & KUZMINA, O.V. (1988): New data on cannizzarite and bursaite. *Neues Jahrb. Mineral., Abh.* **158**, 293-309.

MOZGOVA, N.N., ORGANOVA, N.I., KUZMINA, O.V., BORODAEV, YU.S., LAPUTINA, I.P. & SIVTSOV, A.V. (1984): Homologous series of cannizzarite. *Zap. Vses. Mineral. Obshchest.* **113**, 657-672 (in Russian).

MUMME, W.G. (1976): Proudite from Tennant Creek, Northern Territory, Australia: its crystal structure and relationship with weibullite and wittite. *Am. Mineral.* **61**, 839-852.

MUMME, W.G. (1980): Weibullite $Ag_{0.32}Pb_{5.09}Bi_{8.55}Se_{6.08}S_{11.92}$ from Falun, Sweden: a member of the junoite homologous series. *Can. Mineral.* **18**, 1-12.

MUMME, W.G., TOPA, D. & MAKOVICKY, E. (2009): Proudite: a redetermination of its crystal structure and the proudite–felbertalite homologous series. *Can. Mineral.* **47**, 25-38.

NOWACKI, W. & STALDER, H.A. (1969): Zwei Wismutsulfosalze von Sta. Maria, Val Medel, Kt. Graubünden, Schweiz. *Schweiz. Mineral. Petrogr. Mitt.* **49**, 97-101.

SHANNON, R.D. (1981): Bond distance in sulfides and a preliminary table of sulfide crystal radii. *In* Structure and Bonding in Crystals (M. O'Keeffe & A. Navrotsky, eds.).Academic Press, New York, N.Y. (53-70).

SHELDRICK, G.M. (1997a): SHELXS-97. A *Computer Program for Crystal Structure Determination*. University of Göttingen, Göttingen, Germany.

SHELDRICK, G.M. (1997b): SHELXL-97. *A Computer Program for Crystal Structure Refinement*. University of Göttingen, Göttingen, Germany.

TOPA, D., MAKOVICKY, E. & BALIĆ-ŽUNIĆ, T. (2003): Crystal structures and crystal chemistry of the members of the cuprobismutite homologous series of sulfosalts. *Can. Mineral.* **41**, 1481-1502.

TOPA D., MAKOVICKY, E., CRIDDLE, A.J., PAAR, W.H. & BALIĆ-ŽUNIĆ, T. (2001): Felbertalite, $Cu_2Pb_6Bi_8S_{19}$, a new mineral from the Felbertal scheelite deposit, Austria. *Eur. J. Mineral.* **13**, 961-972.

TRÖMMEL, M. (1981): Abstandskorrelationen bei der Tellur(IV)-Sauerstoff- und bei der Antimon(III)-Sauerstoff-Koordination. *Z. Kristallogr.* **154**, 338-339.

WILLIAMS, T.B. (1986): *An Electron Microscope Study of Non-Commensurate Double-Layer, Heavy-Metal Sulphides*. Ph.D. thesis, The Australian National University, Canberra, A.C.T., Australia.

ZAMBONINI, F., DE FIORE, O. & CAROBBI, G. (1924): Su un solfobismutito di piombo di Vulcano. *Annali R. Osserv. Vesuv., Ser. 3,* **1**, 31-36.

ZHANG, Y., WILKINSON, A.P., LEE, P.L., SHASTRI, S.D., SHU, D., CHUNG, D.-Y. & KANATZIDIS, M.G. (2005): Determining metal ion distributions using resonant scattering at very high-energy *K*-edges: Bi/Pb in $Pb_5Bi_6Se_{14}$. *J. Appl. Crystallogr.* **38**, 433-441.

Received October 25, 2009, revised manuscript accepted May 10, 2010.